Distance and Orientation Dependence of Heterogeneous Electron Transfer: A Surface-Enhanced Resonance Raman Scattering Study of Cytochrome *c* Bound to Carboxylic Acid Terminated Alkanethiols Adsorbed on Silver Electrodes

Lisa A. Dick,† Amanda J. Haes, and Richard P. Van Duyne*

Department of Chemistry, Northwestern University, Evanston, Illinois 60208-3113

Received: August 16, 2000; In Final Form: October 4, 2000

The distance and orientation dependence of the heterogeneous electron-transfer reaction between ferrocytochrome *c* (Fe^{2+}Cc) and a silver film over nanosphere (AgFON) electrode is examined in detail using electrochemical surface-enhanced resonance Raman spectroscopy (SERRS) as a molecularly specific and structurally sensitive probe. The distance between the Fe^{2+} redox center and the electrode surface is controlled by varying the chain length *x* of an intervening carboxylic acid terminated alkanethiol, $HS(CH_2)_xCOOH$, self-assembled monolayer (SAM). The orientation of the heme in Fe^{2+}Cc with respect to the AgFON/$S(CH_2)_x$-COOH electrode surface is controlled by its binding motif. Electrostatic binding of Fe^{2+}Cc to AgFON/$S(CH_2)_x$-COOH yields a highly oriented redox system with the heme edge directed toward the electrode surface. The binding constants were determined to be $K = 5.0 \times 10^6$ M^{-1} and 1.1×10^6 M^{-1}, respectively, for the $x = 5$ and $x = 10$ SAMs. In contrast, covalent binding of Fe^{2+}Cc yields a randomly oriented redox system with no preferred direction between the heme edge and the electrode surface. SERRS detected electrochemistry demonstrates that Fe^{2+}Cc electrostatically bound to the $x = 5$ AgFON/$S(CH_2)_x$COOH surface exhibits reversible oxidation to ferricytochrome *c*, whereas Fe^{2+}Cc electrostatically bound to the $x = 10$ surface exhibits irreversible oxidation. In comparison, Fe^{2+}Cc covalently bound to the $x = 5$ and $x = 10$ surfaces both exhibit oxidation with an intermediate degree of reversibility. In addition to these primary results, the work presented here shows that AgFON/$S(CH_2)_x$COOH surfaces (1) are biocompatible − Fe^{2+}Cc is observed in its native state and (2) are stable to supporting electrolyte changes spanning a wide range of ionic strength and pH thus enabling, for the first time, SERRS studies of these variables in a manner not accessible with either the widely used colloid or electrochemically roughened SERS-active surfaces.

Introduction

Surface-enhanced Raman spectroscopy (SERS) and surface-enhanced resonance Raman spectroscopy (SERRS) are powerful methods for obtaining vibrational spectra from biological molecules.[1−3] The signal enhancement of $\sim 10^6$ at the surface increases sensitivity so that SERS can be used to determine the vibrational information from scarce or low-solubility samples. SERS signals can be further amplified by tuning the laser excitation wavelength λ_{ex} into an electronic absorption band of the target molecule. This provides an additional 10^3-10^4 enhancement from resonance Raman scattering (RRS) which is superimposed on the 10^6 enhancement of SERS to give SERRS. Fluorescence interference, which often obscures Raman scattering in experiments involving biomolecules, is avoided in SERRS due to the strong quenching action of the metal surface. A further strong point of SERRS is that the sample preparation is uncomplicated due to the method's ability to operate on native, unlabeled proteins in aqueous media.

Unfortunately, there are at least two weaknesses of SERRS that currently limit the wider applicability of the technique. First, the adsorption of biological macromolecules at "bare" silver and gold surfaces often results in denaturation so that the resulting SERR spectra are not obtained from biologically functional molecules.[4−6] Fortunately, there are counter examples in which biomolecules in their native states have been observed by SERRS.[7−11] Second, many biophysical studies require the observation of the target molecule over a range of solution conditions such as ionic strength, pH, electrolyte variation, and electrochemical or redox potential. Such studies using SERRS are often compromised because of insufficient stability of colloid or roughened electrode SERS-active surfaces. For example, when using silver or gold colloids, changes in the solution ionic strength, pH, electrolyte, composition, and/or the target biomolecule concentration can cause uncontrollable aggregation of the colloid, which in turn can decrease the enhancement factor by orders of magnitude and thus drastically alter the excitation profile. Consequently, it would be highly desirable to devise a general strategy for fabricating biocompatible SERS-active surfaces that are also as stable as possible to pH, ionic strength, electrolyte variation, and redox potential so that the extraordinary sensitivity and molecular specificity of SERRS and related surface-enhanced spectroscopies could be more generally applied to biological problems.

One approach to the design of a biocompatible electrode surface for SERS is the use of self-assembled monolayers (SAMs) to modify its surface chemistry. This strategy has been successfully employed to provide biocompatible surface environments for applications as diverse as: X-ray diffraction,[12] optical linear dichroism,[13] UV−vis electroreflectance spectroscopy,[14,15] atomic force microscopy (AFM), scanning tunneling

* To whom correspondence should be addressed. E-mail: vanduyne@chem.nwu.edu.

† Present address: 3M, St. Paul, MN.

10.1021/jp0029717 CCC: $19.00
Published on Web 11/05/2000

microscopy (STM),[16,17] ellipsometry,[18,19] electrochemistry,[20−28] neutron diffraction,[29] X-ray standing waves,[30,31] biosensors,[31−34] and metalloprotein nanostructure fabrication.[35] Specific interfacial binding can be maximized by choosing an appropriate terminal functional group for the SAM. Mixed monolayers have even been used to expose functional groups and to promote ionization.[18,36] Their phase separation behavior has been studied quantitatively with atomic resolution STM studies by Weiss, Allara, and co-workers.[37] Overall, the properties of SAMs have been well documented by Raman spectroscopy, ellipsometry, and infrared reflection spectroscopy.[38−41]

The purpose of this paper is to show that appropriately functionalized SAMs in combination with silver film over nanosphere (AgFON) electrodes affect a general solution to the problem of fabricating stable, biocompatible SERS-active surfaces for use in structural studies of surface-confined biomolecules. We illustrate the power of this new approach with an in-depth electrochemical SERRS study of the distance and orientation dependence of the heterogeneous electron-transfer reaction between ferrocytochrome *c* (Fe^{2+}Cc) and a AgFON electrode. AgFON surfaces were chosen because they have surface enhancement factors (EF) as large as 5×10^7 [42] and may be simply fabricated in a highly reproducible manner from readily available materials. The detailed characterization of AgFON and AuFON surfaces with AFM, electrochemistry, and electrochemical SERS of pyridine is the subject of another paper.[43]

Horse heart cytochrome *c* (Cc(horse)) was chosen as the target of this investigation because its vibrational spectroscopy has been thoroughly characterized by RRS, SERRS, and other techniques; thus, a library of data is readily available for comparison.[44−49] Brief reviews of the main structural features of Cc and the results of selected previous investigations of surface-confined Cc, with the emphasis on electrochemistry and SERRS, follow to provide the appropriate context for our work.

Cc is a 12.5 kDa protein that functions as an electron carrier in the electron transport chain of mitochondrial respiration. The molecule is approximately spherical in shape with a 35 Å diameter. Depending on its oxidation state, Cc has an overall dipole moment of 308−325 D.[50] Cc contains a heme that is bound to the protein via two thioether linkages, has a solvent exposed edge, and is surrounded by six lysine residues which are important in binding to its physiological partners.[50] Methionine-80 and histidine-18 serve as the axial ligands of the central Fe so that the low-spin state is inherent to both the oxidized and reduced forms. Cc carries a +9 charge at neutral pH,[51] making it a good candidate for electrostatic binding interactions.

Many studies of Cc bound to bare metal and on SAM coated surfaces have been reported.[20−22,26,28,47,52−54] Several techniques, including SERRS[4,5,8,55−65] have been used for these studies. Distance dependence SERS studies of Cc sandwiched between Ag and Au colloids have been recently reported by Keating et al.[10,11] They found that the Au:Cc system is not destroyed in the presence of Ag aggregates, and that Cc does not change its orientation once Ag is added to the system. By sandwiching the Cc between Au and Ag colloids, they found that they could control the orientation of Cc.[10] Additionally, they compared the wavelength dependence of SERRS spectral intensities for Cc:Au, Cc:Ag, and Ag:Cc:Au sandwiches and found that Cc adsorbed directly to Ag is less likely to experience conformational changes than Cc:Au. For all systems studied, the most intense SERRS signal was measured for the Au:Cc:Ag sandwich.[11]

The heterogeneous electron-transfer kinetics of Cc coupled to carboxylic acid-terminated alkanethiol SAMs on gold (111) electrodes has been studies by Avila et al.[28] Their studies suggest that the electron transfer (ET) between Cc and Au mediated by long alkanethiol chains was very slow and limited by a conformational rearrangement of the Cc. ET for short alkanethiol chains was found to be independent of chain length, ionic strength, and pH.

SERRS and UV−vis electroreflectance spectroscopies have been used to study a related heme protein, cytochrome c_3, immobilized on bare and SAM coated silver electrodes.[66] Because it exhibits reversible voltammetric responses, cytochrome c_3 was chosen for their studies. They found that the protein structure and electrochemical response were strongly dependent on electrode modifications.

SERRS was used to study the structure of Cc bound to hybrid bilayer membranes.[34] They found that as negative potentials were applied, the low-spin conformation of the Cc heme was reduced. This differs from Cc bound to a bare metal electrode in which the high-spin conformation of the heme is reduced.

Despite the extensive work on the electrochemistry and spectroscopy of surface-confined Cc cited above, it is not currently known to what extent its heterogeneous electron transfer dynamics are determined by the distance between the redox center and the electrode surface as compared to their relative orientation. In this paper, we show that both structural factors come into play. The results presented here will convincingly demonstrate that (1) the electrostatic binding of Fe^{2+}Cc to AgFON/$S(CH_2)_x$COOH surfaces yields a highly oriented redox system with the heme edge directed toward the electrode surface; (2) the binding constants were determined to be $K = 5.0 \times 10^6$ M^{-1} and 1.1×10^6 M^{-1}, respectively, for the $x = 5$ and $x = 10$ SAMs; (3) covalent binding of Fe^{2+}Cc yields a randomly oriented redox system with no preferred direction between the heme edge and the electrode surface; and (4) SERRS detected electrochemistry demonstrates that Fe^{2+}Cc electrostatically bound to the $x = 5$ AgFON/$S(CH_2)_x$COOH surface exhibits reversible oxidation to ferricytochrome *c* (Fe^{3+}-Cc), whereas Fe^{2+}Cc electrostatically bound to the $x = 10$ surface exhibits irreversible oxidation and Fe^{2+}Cc covalently bound to the $x = 5$ and $x = 10$ surfaces both exhibit oxidation with an intermediate degree of reversibility. In addition, we will provide evidence that AgFON/$S(CH_2)_x$COOH surfaces are (1) biocompatible as measured by SERRS and the retention of a surface $E°$ value consistent with the native state of Cc and (2) stable to pH, ionic strength, electrolyte, and redox potential variations without changing the surface enhancement factor. This enables, for the first time, SERRS studies of these variables in a manner not accessible with either the widely used colloid or electrochemically roughened SERS-active surfaces.

Experimental Section

Cytochrome *c*. Cytochrome *c* (type IV, horse heart) was purchased from Sigma Chemical Co. and purified.[67] Following purification, it was stored under liquid nitrogen and thawed immediately prior to use. Once diluted to the appropriate concentration, the solution was kept chilled on ice until room-temperature experiments began.

Chemicals. 1-Ethyl-3-(3-(dimethylamino)propyl)carbodiimide hydrochloride (EDC) (Sigma, St. Louis, MO), anhydrous diethyl ether (Fisher Scientific), 6-bromohexanoic acid, 11-bromoundecanoic acid, 1-octanethiol (1-OT), 1-hexanethiol (1-HT), 1-butanethiol (1-BT), and potassium thioacetate (Aldrich Chemical Co., Milwaukee, WI) were used as purchased. Other

chemicals of reagent grade or better were used as received. Water of 18 MΩ resistivity was obtained with a series of purifying cartridges (Milli-Q, Millipore, Marlborough, MA).

SERRS Spectroelectrochemical Instrumentation. The SERRS measurement system consists of an argon ion laser (Spectra Physics model 171−18 or BeamLok 2060), a 1" holographic notch filter (Physical Optics Corp., Torrance, CA), a single-grating monochromator (Acton Research Corp. model VM-505), a liquid N_2 cooled Photometrics PM-512 CCD detector, and a data acquisition system (Photometrics, Tucson, AZ). The spectral positions of the CCD pixels were calibrated using the emission lines of known wavelengths from a Ne lamp. Spectral analysis and data graphics were performed using a combination of commercial software including LabCalc A2.22, Grapher 1.21, and CorelDraw 9.0. Typical conditions for Raman measurements were power = 8 mW, $\lambda_{ex} = 514.5$ nm excitation, 4 cm^{-1} band-pass, and 30−300 s integration times. The visible laser excitation utilized in these studies is in resonance with electronic absorption spectrum of Cc, leading to the acquisition of SERRS. The electrochemical cell[68] and locally constructed potentiostat[69] have been previously described.

AgFON Surface Fabrication. Ag (D. F. Goldsmith, Evanston, IL) electrode substrates were constructed by sealing a Ag wire into a fiberglass body with Torr Seal epoxy (Varian Vacuum Products, Lexington, MA). After curing 24 h in a 40 °C oven, the excess epoxy was mechanically polished with sand paper to expose an electrode. Electrodes were then carefully polished with 5, 1, 0.3, and 0.05 μm alumina/water on a polishing cloth (Buehler Ltd., Lake Bluff, IL). After each step, electrodes were thoroughly rinsed with water and methanol.

AgFON surfaces were fabricated with the use of a modified Consolidated Vacuum Corporation vapor deposition chamber. The steps included: coating a smooth electrode surface with 542 nm diameter polystyrene nanospheres (Interfacial Dynamics Corporation, Portland, OR), masking off the area where metal was not desired, depositing the metal, and removing the mask. Nanospheres were diluted by a factor of 2 in a 1:800 dilution of methanol in TritonX-100. During the deposition, pressures in the diffusion pump chamber were $<10^{-6}$ Torr, and the deposition source was a tungsten boat filled with silver wire. The mass thickness of films was measured with a quartz crystal microbalance which was calibrated by stripping voltammetry[70,71] and with AFM of partially masked samples.

AgFON Surface Modification with SAMs. AgFON electrodes were immersed in ethanolic solutions of ∼1 mM SAM solutions for 2−3 days at room temperature. 11-Mercaptoundecanoic acid (11-MUA) was synthesized according to Troughton et al.[39] and combined in a 1:3 ratio with 1-OT.[39] 6-MHA was synthesized[72] and used alone as well as in combination with 1-BT.

Cross-Linking Conditions. For the covalent studies, a water-soluble, zero length cross-linking agent, EDC, which directly binds COOH and NH functionalities, was employed to bind lysine and arginine groups of Cc with AgFON/SAM surfaces.[22] First, 200 μL of 6×10^{-6} M Cc was incubated for 20 min at a COOH terminated AgFON/SAM. Next, 50 μL of 0.5 M EDC was allowed to react for 30 min. Finally, the surface was thoroughly rinsed with phosphate buffer.

Experimental Solution Conditions. A stock solution of Cc-(horse) was prepared at 1.5×10^{-3} M in 4.4 mM potassium phosphate buffer (KPi), pH 7. Aliquots of this solution were added to degassed 4.4 mM KPi buffer (pH 7) and injected into a potential controlled electrochemical cell. In experiments that involve cross-linking the protein to the AgFON surface, only degassed 4.4 mM KPi buffer (pH 7) was introduced into the cell from the outset. A 0.5 M aqueous potassium hydroxide solution was used to adjust the pH of the 4.4 mM KPi buffer in the pH range from 6 to 9.

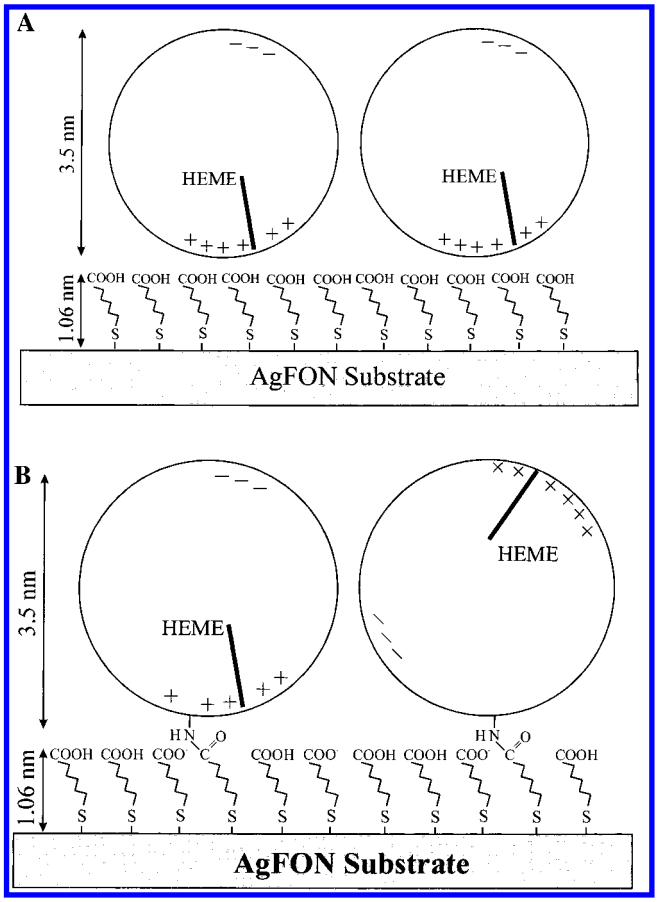

Figure 1. Schematic models of the (A) electrostatic binding motif and (B) covalent binding motif between the positively charged lysine residues near the heme edge of Fe^{2+}Cc and AgFON/6-MHA modified electrodes. The diameter of Fe^{2+}Cc and the 6-MHA chain length are drawn to scale.

Results and Discussion

SERS of SAM/AgFON Surfaces. The electrostatic and covalent binding configurations that were studied in this work are shown schematically in Figure 1A,B, respectively, with the SAM chain length and Cc diameter drawn to scale. SER spectra (data not shown) of SAMs on AgFON surfaces were obtained in several vibrational regions. The most intense and reproducible bands for a series of SAMs are observed in the C−H stretching region. As the number of methylene groups increases, the signal of these overlapping bands in the C−H region intensifies. For mixed monolayers, mercaptocarboxylic acid/alkanethiol, evidence of the methyl-terminated SAM is present by the appearance of the methyl stretch at 2956 cm^{-1}.[38] The spectra obtained for these monolayers are consistent with those obtained in a study presented by Bryant and Pemberton.[38]

Between 300 and 1600 cm^{-1}, where Cc bands appear, SER spectra (data not shown) from SAMs are weak in intensity. The region near 700 cm^{-1} contains conformational information derived from the C−S stretching frequency. For molecules in a trans (T) conformation, the shift is near 700 cm^{-1}, and for those in a gauche (G) conformation, near 630 cm^{-1}. The signals observed in our studies were of molecules in the *T* conformation. Like the observations in the C−H region, these results are

TABLE 1: Normal Mode Assignments, Resonance Raman, and Surface-Enhanced Resonance Raman Frequencies of Nickel(II) Octaethylporphyrin (NiOEP) and Ferrocytochrome *c* (Fe^{2+}Cc)

symmetry class (D_{4h})	mode no.	RRS[a] (NiOEP)	RRS[a] (Cc)	SERRS[b] (Cc)	local coordinate[a,c]
A_{1g}	ν_3	1520	1496	1494	$\nu(C_\alpha-C_m)_{sym}$
	ν_4	1364	1362	1361	ν(pyr half-ring)$_{sym}$
	ν_6	804	796	796	ν(pyr breathing)
B_{1g}	ν_{10}	1655	1626	1623	$\nu(C_\alpha-C_m)_{asym}$
	ν_{11}	1577	1551	1545	$\nu(C_\beta-C_\beta)$
	ν_{13}	1220	1232	1225	$\delta(C_m-H)$
	ν_{15}	751	750	750	ν(pyr breathing)
A_{2g}	ν_{19}	1603	1587	1585	$\nu(C_\alpha-C_m)_{asym}$
	ν_{20}	1393	1400	1397	ν(pyr quarter-ring)
	ν_{21}	1307	1314	1308	$\delta(C_m-H)$
	ν_{22}	1121	1130	1120	ν(pyr half-ring)$_{asym}$
B_{2g}	ν_{30}	1159	1174	1170	ν(pyr half-ring)$_{sym}$
	ν_{31}	1015	1032	1025	$\nu(C_\beta-C_1)_{asym}$
E_u	ν_{46}	927	925	921	δ(pyr deform)$_{asym}$
	ν_{50}	358	360	362	M−N
	ν_{51}	328	309	310	$\delta(C_\beta-C_1)_{asym}$
			Substituent Modes		
		1025	969	967	$\nu(C_c-C_d)_{6,7}$
A_{2u}	γ_4	844	826	826	$\gamma(C_m-H)$
		378	372	374	$\delta(C_\beta$-C_c-$C_d)_{6,7}$

[a] Hu et al. *J. Am. Chem. Soc.* **1993**, *115*, 12446−12458. [b] This work. [c] Li et al. *J. Phys. Chem.* **1990**, *94*, 47−61.

consistent with those obtained by Pemberton. Peaks at 894 and 1070 cm^{-1} were not always apparent. The peak near 1070 cm^{-1} has been assigned to ν(C−C) for molecules in the *T* conformation. In this region, our results are similar to other carboxylic acid monolayer studies by Maeda et al.[73] and are much less resolved than 1-alkanethiol studies by Pemberton.

RRS of Fe^{2+}Cc in Solution Compared with SERRS of Fe^{2+}Cc Adsorbed on Electrochemically Roughened Silver Electrodes. The solution phase RR spectrum of Fe^{2+}Cc has been thoroughly studied[74,75] by Spiro and co-workers. Detailed normal mode assignments have been made using normal coordinate analysis, spectral comparisons with model compounds such as nickel octaethylporphyrin (NiOEP), and the analysis of isotopically labeled species.[48] Table 1 summarizes these assignments and the observed RR frequencies for NiOEP and Fe^{2+}Cc. The Q-band excited (λ_{ex} = 514.5 nm) RR spectrum of 5.5×10^{-4} M Fe^{2+}Cc purified in our laboratory and dissolved in aqueous buffer solution is shown in Figure 2A. The frequencies of the nine vibrational lines observed in the 1000−1650 cm^{-1} range of this spectrum closely match those in the literature (Table 1) and are well-resolved with symmetric line shapes, and have narrow line widths (fwhm) $\Gamma \sim 10$ cm^{-1}. Intense scattering from both nontotally symmetric (B_{1g}, A_{2g}, and B_{2g}) and symmetric modes is observed as expected.

The Q-band excited (λ_{ex} = 514.5 nm) SERR spectrum of 1.0×10^{-6} M Fe^{2+}Cc spontaneously adsorbed at a silver electrode roughened electrochemically by successive oxidation−reduction cycles (AgORC) is shown in Figure 2B. Thirteen vibrational lines are observed in this spectrum and are equivalent to that published earlier by Cotton et al.[4] but have far weaker intensities than the Soret-band excited (λ_{ex} = 413 and 457 nm) SERR spectra of Fe^{2+}Cc reported by Hildebrandt and Stockburger.[76,77] Nine of the vibrational lines observed in Figure 2B are readily matched with those observed in the solution RR spectrum in the 1000−1650 cm^{-1} range; however, the bands at 1025, 1198, and 1438 cm^{-1} in the surface SERR spectrum are not seen in the solution RR spectrum. The 1025 cm^{-1} is taken to be the SERRS counterparts of the ν_{31} (B_{2g}) RR mode at 1032 cm^{-1} while, the origin of the 1198 and 1438 cm^{-1} bands is not known. There are marked differences in the relative intensity patterns, line shapes, and line widths between the RR and AgORC SERR spectra of Fe^{2+}Cc. For example, the most intense peak in the solution RR spectrum is the ν_{21} (A_{2g}) mode at 1313 cm^{-1} while at the electrode the most intense peak is either the ν_4 (A_{1g}) mode at 1360 cm^{-1} or the ν_{19} (A_{2g}) mode at 1585 cm^{-1}. With regard to the difference in line shapes, the baseline-resolved RR triplet ν_{16} (B_{1g}) 1622 cm^{-1}, ν_{19} (A_{1g}) 1585 cm^{-1}, and ν_{11} (B_{1g}) 1547 cm^{-1}, is not well-resolved in AgORC SERRS. Similarly, the RR line widths in solution have broadened by a factor of 1.5−2.0 in AgORC SERRS.

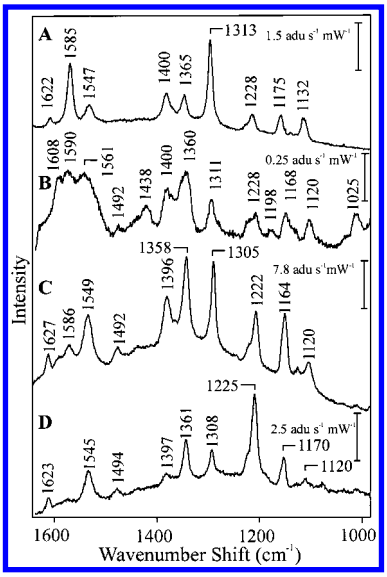

Figure 2. Comparison of RRS of Fe^{2+}Cc in solution with SERRS of Fe^{2+}Cc adsorbed at various Ag surfaces. (A) RRS obtained from 5.5×10^{-4} M Fe^{2+}Cc in 20 mM KPi, pH 6.5 solution, spinning tube. (B) SERRS from Fe^{2+}Cc at a "bare" AgORC electrode (0.5 V to −0.5 V vs Ag/AgCl step, 25 mC cm^{-2}), 1×10^{-6} M in 10 mM Na_2SO_4, pH 7.0, $E_{applied}$ = −0.4 V vs Ag/AgCl, spontaneous adsorption. (C) SERRS from Fe^{2+}Cc at a "bare" AgFON electrode, 1.0×10^{-6} M Fe^{2+}Cc in 4.4 mM KPi, pH 7.0, $E_{applied}$ = −0.4 V vs Ag/AgCl, spontaneous adsorption. (D) SERRS from Fe^{2+}Cc at a AgFON/6-MHA surface, 1.0×10^{-6} M Fe^{2+}Cc in 4.4 mM KPi, pH 7.0, $E_{applied}$ = −0.4 V vs Ag/AgCl, electrostatic binding. Experimental conditions: 8 mW at λ_{ex} = 514.5 nm.

The difference in the relative intensity patterns of a solution RR spectrum and its surface-enhanced counterpart are a consequence of the selection rules[78−83] for surface-enhanced spectroscopies. The intensities in both SERS and SERRS are

determined by the relative orientation of the vibrational eigenvectors of the adsorbate and the orientation of the local electromagnetic fields (always perpendicular to the surface—Gauss' law) responsible for the surface enhancement resulting in preferential enhancement of modes oriented perpendicular to the surface. Since the assigned vibrational modes of $Fe^{2+}Cc$ in the 1000−1650 cm^{-1} range are all associated with the heme, one can conclude that the relative intensity pattern of SERR spectrum of $Fe^{2+}Cc$ compared to its RR spectrum contains information about the angle between the heme and the surface normal. Natan and co-workers have recently discussed the pros and cons of using the B_{1g}/A_{1g} SERRS intensity ratio for the determination of heme orientation in adsorbed Cc.[10,11] The line-shape and line-width differences as well as the origin of the 1438 cm^{-1} band in the AgORC SERRS are plausibly the result of irreversible changes in the secondary or tertiary structure of adsorbed $Fe^{2+}Cc$ (viz., denaturation) caused by direct interactions between the "bare" silver surface and the adsorbed protein. Despite the differences noted above, the strong similarity between these solution RR and surface SERR spectra argues against the complete unfolding of adsorbed $Fe^{2+}Cc$ under these conditions.

RRS of $Fe^{2+}Cc$ in Solution Compared with SERRS of $Fe^{2+}Cc$ Adsorbed at AgFON Electrodes. The Q-band excited (λ_{ex} = 514.5 nm) SERR spectrum of 1.0×10^{-6} M $Fe^{2+}Cc$ spontaneously adsorbed at a "bare" AgFON electrode surface is shown in Figure 2C. It exhibits substantial intensity, line-shape, and line-width differences compared with the SERR spectrum of $Fe^{2+}Cc$ on the AgORC surface (Figure 2B). First, the overall intensity in Figure 2C is ∼ 30 times that in Figure 2B, the relative intensities of the 1358 and 1305 cm^{-1} lines are approximately equal, and they are the dominant lines in the spectrum. Furthermore, the SERR spectrum of adsorbed Fe^{2+}-Cc on the "bare" AgFON surface shows vibrational bands with symmetric line shapes, $\Gamma \sim 10$ cm^{-1}, and are as well-resolved as those in the solution RR spectrum. From the line shapes and line widths, we conclude that this SERR spectrum is that of adsorbed $Fe^{2+}Cc$ that is not substantially denatured. Evidently, the more gently contoured surface nanostructure of the AgFON electrode[42] is less aggressive toward denaturation than the AgORC surface which is likely to have significant numbers of adsorbed silver clusters, (Ag_n $4 < n < 10$).[84] From the relative intensity pattern which is similar, but not identical, to that of the solution RR spectrum, we conclude that $Fe^{2+}Cc$ adsorbed at a "bare" AgFON electrode surface is randomly oriented. This latter conclusion is further supported by the relative intensity pattern of the SERR spectra for $Fe^{2+}Cc$ electrostatically bound to carboxylic acid terminated alkanethiol SAM modified AgFON electrodes (vide infra).

RRS of $Fe^{2+}Cc$ in Solution Compared with SERRS of $Fe^{2+}Cc$ Electrostatically Bound to AgFON/6-MHA Electrodes. The Q-band excited (λ_{ex} = 514.5 nm) SERR spectrum of 1.0×10^{-6} M $Fe^{2+}Cc$ electrostatically bound to a AgFON/6-MHA electrode surface is shown in Figure 2D. Ionic strength "jump" experiments will be used to prove the existence of electrostatic binding between $Fe^{2+}Cc$ and the AgFON/6-MHA electrode surface (vide infra). The overall intensity of the SERR signals in Figure 2D is ∼3 times weaker than that in Figure 2C. This is an anticipated consequence of the strong distance dependence of SERS in which signal intensity drops by a factor of 10 for each ∼1.5 nm increment of the Raman chromophore from the surface.[85,86] The factor of ∼3 decrease in SERR intensity between Figures 2C and 2D is consistent with the structural expectation that the heme edge for electrostatically bound $Fe^{2+}Cc$ is spaced away from the Ag surface ∼ 1 nm by the 6-MHA SAM (Figure 1A). The average heme to surface distance is likely to be less than 1 nm for the randomly oriented, spontaneously adsorbed $Fe^{2+}Cc$ in Figure 2C even though there will be a distribution of heme to surface distances due to the existence of rotational disorder.

The relative intensity pattern of Figure 2D is dramatically different than that in Figures 2A-C. For example, the ν_{13} (B_{1g}) mode at 1225 cm^{-1} band is the most intense feature in Figure 2D and the ν_{19} (A_{2g}) mode at ∼1585 cm^{-1},which is the second most intense feature in the solution RR spectrum, is virtually absent. As in Figures 2B and 2C, the vibrational bands in Figure 2D have symmetric line shapes, $\Gamma \sim 10$ cm^{-1}, and are well-resolved. From the line-shape and line-width results, we conclude that electrostatically bound $Fe^{2+}Cc$ is not denatured and from the relative intensity pattern, that it is oriented heme edge toward the Ag surface. Thus, the well-ordered AgFON/SAM surface serves two functions: (1) it protects $Fe^{2+}Cc$ from direct contact with the metal surface thereby eliminating the spectre of denaturation and (2) it orients $Fe^{2+}Cc$ in a manner that is most advantageous for carrying out the function of exchanging electrons with the Ag electrode surface.

Ionic Strength Dependence as a Probe of Binding Interactions between $Fe^{2+}Cc$ and AgFON/6-MHA. The ionic strength of the supporting electrolyte was varied to prove the existence of electrostatic binding between $Fe^{2+}Cc$ and the AgFON/6-MHA electrode surface. In addition, one can demonstrate subtle changes in SAM conformation that occur in response to ionic strength changes. Figure 3A,B show a dramatic variation in the $Fe^{2+}Cc$ SERR intensity at a AgFON/6-MHA surface in a 4.4 mM KPi electrolyte solution in the absence and presence of 0.8 M KCl, respectively. At high ionic strength, the electrolyte screens the Coulombic attraction between the negatively charged carboxylate monolayer and the positively charged lysines near the heme edge of $Fe^{2+}Cc$, leaving no detectable SERR signal from irreversibly bound protein. Similarly, Figure 3C,D compare the SERR spectra of covalently bound $Fe^{2+}Cc$ in the absence and presence of 0.8 M KCl at a AgFON/6-MHA surface. The nearly identical spectra obtained demonstrate the following: (1) the enhancement factor of the AgFON/6-MHA surface is not altered by the introduction of a high ionic strength electrolyte medium and (2) there is little or no electrostatically bound Fe^{2+}-Cc remaining after covalent cross-linking of $Fe^{2+}Cc$ to the AgFON/6-MHA surface via amide bond formation. Our results are in agreement with an electrochemical study conducted under similar conditions.[21,22]

By systematically changing the ionic strength of the buffer, we are able to delicately probe some subtle features of the electrostatic interaction between $Fe^{2+}Cc$ and the AgFON/6-MHA surface. Figure 4 illustrates the SERR spectral changes that occur in the 300−800 cm^{-1} region when the ionic strength is increased by changing the concentration of KPi from 20 to 100 mM and then to 200 mM. While the overall signal intensity does not change, the AgFON/6-MHA/$Fe^{2+}Cc$ system does exhibit reversible changes in its SERR spectrum as a consequence of increasing the ionic strength. The SER intensity of the 700 cm^{-1} C−S stretch from the trans conformer of the SAM is independent of electrolyte ionic strength and may, therefore, be used as an internal standard. Under low KPi conditions, the SERR intensity of the ν_{15} (B_{1g}) of $Fe^{2+}Cc$ at 750 cm^{-1} band is greater than the SER intensity of the 700 cm^{-1} C−S stretch of the SAM. At 100 mM KPi, the intensity of the $Fe^{2+}Cc$ 750 cm^{-1} band decreases to about $^1/_4$ the intensity of the C−S band and at 200 mM, the 750 cm^{-1} band completely vanishes. Similar

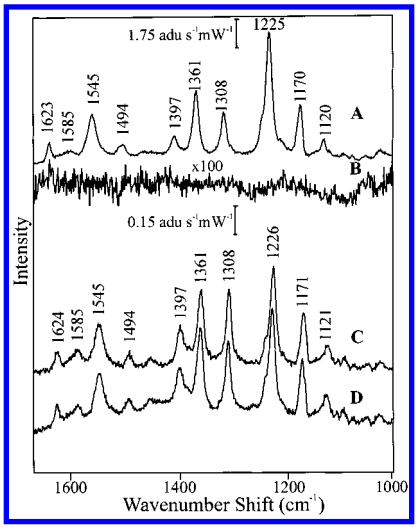

Figure 3. Comparison of SERRS from electrostatically and covalently bound Fe^{2+}Cc at a AgFON/6-MHA surface. (A) electrostatic binding, no added KCl. (B) electrostatic binding, 0.8 M KCl added. (C) covalent binding, no added KCl. (D) covalent binding, 0.8 M KCl added. Experimental conditions: 8 mW at $\lambda_{ex} = 514.5$ nm, 1×10^{-6} M Fe^{2+}-Cc in 4.4 mM KPi, pH 7.0, $E_{applied} = -0.4$ V vs Ag/AgCl.

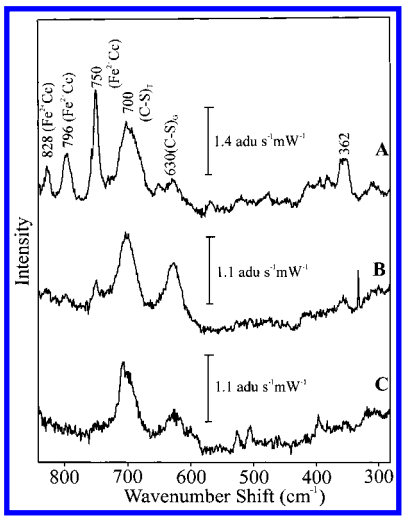

Figure 4. Ionic strength dependence of SERRS from electrostatically bound Fe^{2+}Cc at a AgFON/6-MHA surface. (A) 20 mM KPi buffer, (B) 100 mM KPi buffer and (C) 200 mM KPi buffer. Experimental conditions: 8 mW at $\lambda_{ex} = 514.5$ nm, 1×10^{-6} M Fe^{2+}Cc in 4.4 mM KPi, pH 7.0, $E_{applied} = -0.4$ V vs Ag/AgCl.

intensity variations are observed for the ν_6 (A_{1g}) ring mode at 796 cm^{-1} and the γ_4 (A_{2u}) substituent mode at 828 cm^{-1} of Fe^{2+}Cc.

Even though the SER intensity of the 700 cm^{-1} C−S stretch from the trans (T) conformer of the SAM is independent of electrolyte ionic strength, there are ionic strength induced changes in the intensity of the C−S stretch from the gauche (G) conformer. The low and high ionic strength spectra have similar contributions from the *T* (700 cm^{-1}) and G (630 cm^{-1}) conformations of the SAM, but the G contribution is much larger in the presence of the intermediate strength buffer. Possibly, the low and high ionic strength conditions keep the SAM monolayer ordered (with high and no Fe^{2+}Cc coverages, respectively). At the intermediate ionic strength, the appears to be some conformational flexibility in the methylene chain of the SAM that may reflect the existence of surface domain structures where Fe^{2+}Cc is electrostatically bound and other domains where it is not.

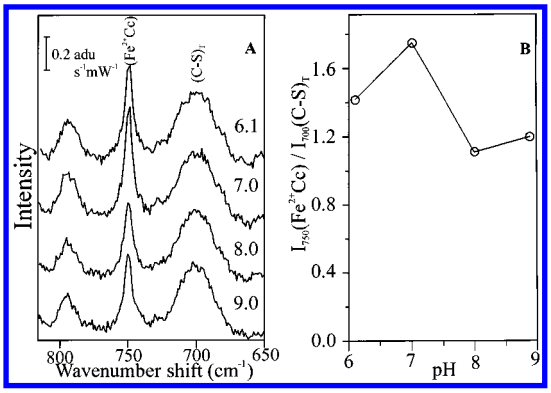

Figure 5. pH dependence of SERRS from electrostatically bound Fe^{2+}-Cc at a AgFON/6-MHA surface. (A) 650 cm^{-1} − 850 cm^{-1} range, pH = 6.1, 7.0, 8.0, and 9.0. (B) SERR intensity of Fe^{2+}Cc 750 cm^{-1} mode normalized to the SER intensity of the $(C-S)_T$ stretch of AgFON/6-MHA as a function of pH. Experimental conditions: 8 mW at $\lambda_{ex} = 514.5$ nm, 1×10^{-6} M Fe^{2+}Cc in 4.4 mM KPi, $E_{applied} = -0.4$ V vs Ag/AgCl.

In summary, we have demonstrated, for the first time, that the enhancement factors of a SAM-modified AgFON surface do not change with ionic strength permitting the systematic study of this important biophysical variable in the context of SERRS.

pH Dependence as a Probe of Binding Interactions between Fe^{2+}Cc and AgFON/6-MHA. Using the carboxylic acid terminated SAM spacer to bind Fe^{2+}Cc to a AgFON surface has a possible disadvantage. Near pH 4, the protein is in its most stable form, but the carboxylic acid groups may be protonated. From contact angle measurements[87] and quartz crystal microbalance frequency changes,[88] the surface pK_as for carboxylic acid terminated alkanethiol SAMs have been determined. While the pK_a of the corresponding solution species is typically between pH 3 and pH 4, the surface pK_as were between 7 and 10. Also, the transition from COOH to COO^- for the surface species occurs over a range of 3−4 pH units, whereas for the solution species, the transition occurs within 1 pH unit. Furthermore, it was found that the surface ionization state is dependent upon SAM chain length, composition, hydrogen bonding interactions, and electrostatic interactions. Possibly, the hydrogen bonding interactions between neighboring headgroups in the SAM make it difficult for ionization to occur at low pHs. We estimate that approximately 10% of the headgroups are ionized at pH 7. A higher degree of ionization may be obtained by exposing the monolayer to higher pH conditions.

From the protein point of view, however, higher pH can lead to instability. As the isoelectric point (pI) is approached, the net charge is decreased to zero and the protein becomes insoluble in water. Additionally, as the overall charge on Cc is decreased, its affinity for the negatively charged surface decreases. This instability problem can be overcome by maintaining solution conditions at least one pH unit below the pI of the protein.

A pH titration was performed to test the relationship between SAM ionization and Fe^{2+}Cc charge. Figure 5 illustrates spectra taken between pH 6 and 9 and reports the changes in Fe^{2+}Cc SERRS intensity versus the constant SERS intensity of the *T* (700 cm^{-1}) C−S mode in the 6-MHA SAM. As the pH changes from 6 to 7, the protein remains positively charged and the monolayer is ionized. This leads to an increase in SERRS intensity. The monolayer continues to ionize further between pH 7 and 8, but the protein loses a significant portion of its overall charge because fewer molecules are bound to the surface. This leads to a decrease in Fe^{2+}Cc SERRS intensity. From pH 8 to 9, the protein and SAM are ionized to equal extents thus producing a fairly constant signal intensity.

Our results do not agree with a previous study of a cysteine monolayer and Cc on colloidal Ag.[89] As pH was increased between 8 and 10, a 0.5 unit width transition at pH 9 was observed. The authors argued that cysteine is uncharged at neutral pH and upon loss of a proton near the pK_a of the amino group (10.8 in neutral solution), Cc adsorbed to the negatively charged surface. Although we cannot argue with the result, there may be alternative explanations. First, if the surface bound amino group follows the same behavior as the surface bound carboxylic acid group, it will not deprotonate until 3 pH units larger than the solution value, that is, around pH 13. Next, it is unlikely that Cc retains an appreciable positive charge as its pI is approached (between pH 9 and 10). This increased signal intensity may be explained by protein denaturation. As the pI is approached, the heme group is allowed to closely approach the surface or many isolated heme groups are allowed to approach the surface instead of a lesser number of intact Cc molecules.

Our results can also be compared to those obtained by Macdonald and Smith.[57] In their study of Ag-citrate colloidal particles, a pH dependence was observed for υ_{10} (1640 cm^{-1}) versus υ_4 (1375 cm^{-1}) of Fe^{3+}Cc. As pH was increased, υ_{10} grew in relative intensity, leading the authors to conclude that slight realignment of the protein was responsible for the signal increase. In contrast, the same ratio for Fe^{2+}Cc at the carboxylic acid-terminated AgFON/6-MHA surface of our studies does not show an increase, but rather, displays pH independence. The only mode which exhibited a pH dependence at the MFON/6-MHA surface was the 1225 cm^{-1} B_{1g} vibration. As the pH was increased, the SERR intensity of the 1225 cm^{-1} band decreased relative to all other bands. We interpret this pH dependent intensity pattern as a consequence of the heme being highly rotationally ordered and nearly perpendicular to the AgFON surface at low pH and more disordered at higher pH values.

Measurement of the Electrostatic Binding Constant between Fe^{2+}Cc and AgFON/SAM Surfaces Using SERRS-Detected Titrations. In addition to our goals of fabricating a SERS-active surface that (1) exhibited strong, stable surface enhancement and (2) prevented loss of biological function by protein denaturation, we sought to create a surface that was biomimetic in the sense that it behaved in a manner analogous to the natural Cc binding partner(s) in electrostatic protein−protein complexes. Such protein−protein interactions are of manifest importance in the area of interprotein electron transfer. The prototypical protein complex for the study of interprotein electron transfer has been the Cc−Cc peroxidase (CcP) complex. Thus, in the context of the present SERRS study of the electrostatic binding between Fe^{2+}Cc and AgFON/SAM surfaces, the question naturally arises as to the magnitude of the association binding constant in comparison to that of the native Cc-CcP system. Systematic studies of the Cc−CcP system by Hoffman and co-workers have demonstrated that the association binding constant for 1:1 complex is ~10^6 M^{-1} at 10 mM KPi and pH 7.[90,91]

SERRS-detected binding titration curves were measured for the 11-MUA/1-OT, 6-MHA, and 6-MHA/1-BT surfaces by monitoring the increase in the intensity of a selected vibrational mode of Fe^{2+}Cc as a function of its concentration. Figure 6 shows the binding curve for Fe^{2+}Cc interacting with the 11-MUA/1-OT monolayer as measured by the intensities of the ν_4 (A_{1g}) mode at 1361 cm^{-1} and the ν_{21} (A_{2g}) mode at 1308 cm^{-1} band as a function of [Fe^{2+}Cc]. It should be noted that the Q-band excited (λ_{ex} = 514.5 nm) SERR spectrum (data not shown) of 1.0 × 10^{-6} M Fe^{2+}Cc electrostatically bound to the

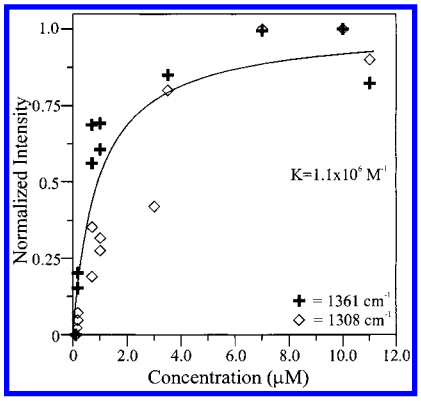

Figure 6. SERRS-detected electrostatic binding titration curve for Fe^{2+}-Cc on a AgFON/11-MUA/1-OT surface. (+) 1361 cm^{-1} band, (◇) 1308 cm^{-1} band, and the line is a Langmuir adsorption isotherm with K = 1.1 × 10^6 M^{-1}. Experimental conditions: 8 mW at λ_{ex} = 514.5 nm, 1 × 10^{-6} M Fe^{2+}Cc in 4.4 mM KPi, pH 7.0, $E_{applied}$ = −0.4 V vs Ag/AgCl.

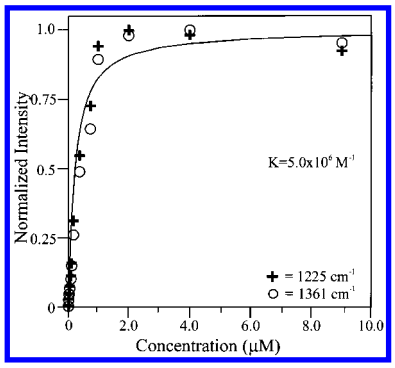

Figure 7. SERRS-detected electrostatic binding titration curve for Fe^{2+}-Cc on a AgFON/6-MHA/1-BT surface. (+) = 1225 cm^{-1} band, (◇) 1361 cm^{-1} band, and the line is a Langmuir adsorption isotherm with K = 5.0 × 10^6 M^{-1}. Experimental conditions: 8 mW at λ_{ex} = 514.5 nm, 1 × 10^{-6} M Fe^{2+}Cc in 4.4 mM KPi, pH 7.0, $E_{applied}$ = −0.4 V vs Ag/AgCl.

AgFON/11-MUA/1-OT electrode surface is similar, except for the overall intensity and the relative intensity pattern, to that shown in Figure 2D for the AgFON/6-MHA surface. The overall intensity of the SERR signals at saturation coverage for Fe^{2+}-Cc bound to the AgFON/11-MUA/1-OT electrode surface is ~10 times weaker than that for the AgFON/6-MHA electrode surface in Figure 2D. This decrease in overall intensity and the variation in relative intensity pattern is a consequence of the SERS distance dependence and will be discussed in detail in another paper.[92] The SERR signal intensities shown in Figure 6 increase sharply over the interval between 1 × 10^{-7} M and 8 × 10^{-6} M Cc, after which no signal increase is observed. The Langmuir adsorption isotherm, which assumes no lateral interactions between adsorbed Fe^{2+}Cc molecules, is used to estimate the binding constant. Using a binding constant of 1.1 × 10^6 M^{-1}, a reasonable fit to the observed data was obtained.

Figure 7 shows the binding curve for Fe^{2+}Cc interacting with the 6-MHA/1-BT monolayer as measured by the intensities of the ν_4 (A_{1g}) mode at 1361 cm^{-1} and the ν_{13} (B_{1g}) mode at 1225 cm^{-1} band as a function of [Fe^{2+}Cc]. The AgFON/6-MHA/1-BT surface quickly reached saturation at approximately 2 × 10^{-6} M. Similar binding interactions were observed for the undiluted 6-MHA monolayer. Using a binding constant of 5.0 × 10^6 M^{-1}, a reasonable fit to the observed data was obtained. From the SERRS-detected titration data presented here, we conclude that electrostatic binding between Fe^{2+}Cc and AgFON/SAM surfaces is biomimetic to the extent that the magnitude

TABLE 2: Comparison of Oxidation State Markers for Cytochrome *c* in Solution and at AgFON and AgFON−SAM Electrodes

symmetry class	mode no.	RRS		SERRS (AgFON)[a]		SERRS (AgFON−SAM)	
		Fe^{2+}	Fe^{3+}	Fe^{2+}	Fe^{3+}	Fe^{2+}	Fe^{3+}
A_{1g}	ν_3	1496	1502	1492	(1492)	1494	(1494)
	ν_4	1362	1374	1359	1371	1361	(1361)
B_{1g}	ν_{10}	1626	1636	1627	1640	1623	1638
	ν_{11}	1551	1562	1550	1563	1545	(1545)

[a] SERRS signal intensity drops upon changing the applied potential from −0.4 V to 0.0 V, where Fe^{3+} should be the species present. Parentheses indicate that the last signal detected was at the noted location.

of the association binding constant is of comparable magnitude to that of the native Cc−CcP system.[90,91]

One further observation concerning the SERRS-detected titration data should be pointed out. In our experiments, the intensities of all the vibrational modes increased uniformly as concentration of Fe^{2+}Cc was increased. This is in contrast to the study published by Macdonald and Smith[57] in which they observed that the ratio of ν_{10}/ν_4 increased as the concentration of Fe^{2+}Cc was increased. From this, they concluded that Fe^{2+}-Cc binds to the surface with an angular dependence.

SERRS Spectroelectrochemistry of Fe^{2+}Cc/SAM/AgFON. In this section we provide detailed evidence that 6-MHA/AgFON surfaces are biocompatible as measured by SERRS spectroelectrochemistry experiments. Specifically, we will demonstrate the reversibility of the one-electron redox reaction:

$$\text{AgFON/6-MHA/Fe}^{3+}\text{Cc}_{\text{surf}} + 1\text{e}- \rightleftharpoons \text{AgFON/6 - MHA/Fe}^{2+}\text{Cc}_{\text{surf}} \quad (1)$$

and calculate its surface formal potential when the redox partners are electrostatically bound to the surface. In addition, we will show the extent to which eq 1 is irreversible when the redox partners are electrostatically bound to the AgFON/11-MUA/1-OT surface or covalently bound to either AgFON/SAM surface.

Potential Dependence of the Oxidation and Spin State Marker Band Frequencies. One criterion for confirming the retention of biological function for surface-confined Fe^{2+}Cc is the reversible SERRS detection of the oxidation state marker bands for Cc.[93] Table 2 lists the literature values for the solution RRS oxidation state marker bands along with our SERRS results. Four oxidation state marker bands are readily observed in solution RRS studies for Fe^{2+}Cc: ν_4 (A_{1g}) 1362 cm^{-1}, ν_3 (A_{1g}) 1496 cm^{-1}, ν_{11} (B_{1g}) 1551 cm^{-1}, and ν_{10} (B_{1g}) 1626 cm^{-1}. When oxidized to Fe^{3+}Cc, these bands shift to 1374, 1502, 1562, and 1636 cm^{-1}, respectively.

These same four oxidation state marker bands are observed in the SERR spectrum of Fe^{2+}Cc adsorbed at a "bare" AgFON electrode surface (Figure 2C). At −0.4 V versus Ag/AgCl the Fe^{2+} marker bands appear at 1358, 1492, 1549, and 1627 cm^{-1} and differ only slightly in frequency from solution RRS measurements indicating that the heme Fe is in its reduced state. As the potential is scanned to more positive values, the overall SERR signal intensity decreases, but three of the Fe^{3+} oxidation state marker bands that are clearly seen at 1371, 1563, and 1640 cm^{-1} are fully developed at the anodic potential of +0.10 V versus Ag/AgCl. The fourth oxidation state marker is too weak to be observed at this potential. While the observed frequency shifts were reversible as the potential was again scanned cathodically to −0.4 V versus Ag/AgCl, the intensity was not (vide infra).

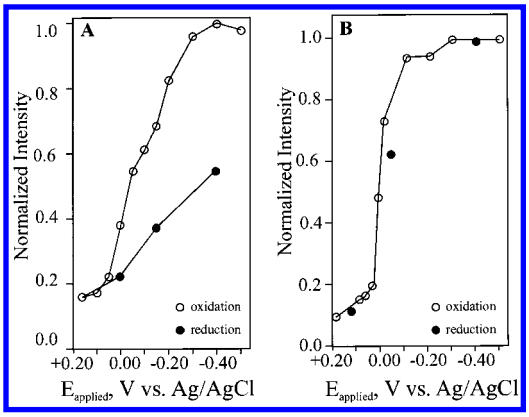

Figure 8. SERRS-detected steady-state voltammetry for adsorbed Fe^{2+}-Cc as monitored by the intensity of the 1225 cm^{-1} mode. (A) "bare" AgFON electrode, spontaneous adsorption. (B) AgFON/6-MHA/Fe^{2+}-Cc, electrostatic binding. Anodic scan direction (open circles) and cathodic scan direction (filled circles). Experimental conditions: 8 mW at λ_{ex} = 514.5 nm, 1×10^{-6} M Fe^{2+}Cc in 4.4 mM KPi, pH 7.0, −0.50 V ≤ $E_{applied}$ vs Ag/AgCl ≤ +0.20 V.

Similarly, these four oxidation state marker bands are observed in SERR spectrum of Fe^{2+}Cc electrostatically bound to a AgFON/6-MHA surface (Figure 2D). At −0.4 V versus Ag/AgCl the Fe^{2+} marker bands appear at 1361, 1494, 1545, and 1623 cm^{-1}. As a result of the strong SERRS distance dependence, the only oxidation marker that could be clearly observed for Fe^{3+}Cc at +0.1 V versus Ag/AgCl was the ν_{10} (B_{1g}) mode which shifted to 1638 cm^{-1}. In this case, both the frequency shifts and intensities were fully reversible as the potential was scanned cathodically to −0.4 V versus Ag/AgCl.

In addition, only one spin state marker band could be observed in the SERR spectrum of Fe^{2+}Cc electrostatically bound to a AgFON/6-MHA surface (Figure 2D). At −0.4 V versus Ag/AgCl the n_3 (A_{1g}) mode is observed at 1494 cm^{-1} indicating that Fe^{2+}Cc is in the six-coordinate low spin (6cLS) state characteristic of the native protein.[76] Unfortunately, it was not possible to observe this mode upon oxidation at +0.1 V versus Ag/AgCl so that we cannot comment on retention of the 6cLS state in Fe^{3+}Cc.

SERRS-Detected Steady-State Voltammetry. In these experiments, the potential applied to the AgFON or AgFON/SAM electrode was step-scanned from the initial potential, E_1 = −0.4 V versus Ag/AgCl, to the switching potential, E_2 = +0.1 V versus Ag/AgCl, and back to E_1 in ∼100 mV increments. After each 100 mV increment, the potential was held until the SERR intensity reached steady state. Figure 8A shows the SERRS-detected steady-state voltammogram for the oxidation and rereduction of Fe^{2+}Cc adsorbed at a "bare" AgFON electrode surface as monitored by the SERR intensity of the ν_{13} (B_{1g}) mode at 1225 cm^{-1}. This band was chosen for SERRS-detected voltammetry because it is the most intense signal from Fe^{2+}Cc at the AgFON/6-MHA surface with which these data will be compared in Figure 8B. Clearly, the steady-state SERRS voltammogram in Figure 8A **is not reversible**. In contrast, the steady-state SERRS voltammogram of Fe^{2+}Cc electrostatically bound at the AgFON/6-MHA electrode surface shown in Figure 8B **is reversible**.

Surface Formal Potential. The reversible character of the steady state SERRS voltammogram for the electrostatically bound AgFON/6-MHA/Fe^{2+}Cc system allows us to construct a Nernst Plot (Figure 9) from the data in Figure 8B. At applied potentials, $E_{applied} \geq$ -0.4 V versus Ag/AgCl, the electrostatically bound Cc is completely reduced and the ratio of the surface concentrations of oxidized to reduced Cc is $[Fe^{3+}Cc]_{surf}/[Fe^{2+}$-

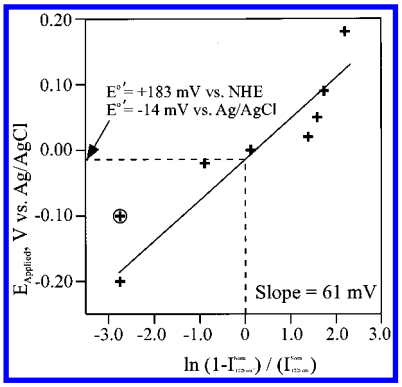

Figure 9. SERRS-detected Nernst plot of electrostatically bound AgFON/6-MHA/Fe^{2+}Cc. The data points from Figure 8B are fit by a line with a slope of 61 mV. The circled point was excluded as an outlier. Experimental conditions: 8 mW at $\lambda_{ex} = 514.5$ nm, 1×10^{-6} M Fe^{2+}-Cc in 4.4 mM KPi, pH 7.0, -0.50 V $\leq E_{applied}$ vs Ag/AgCl $\leq +0.20$ V.

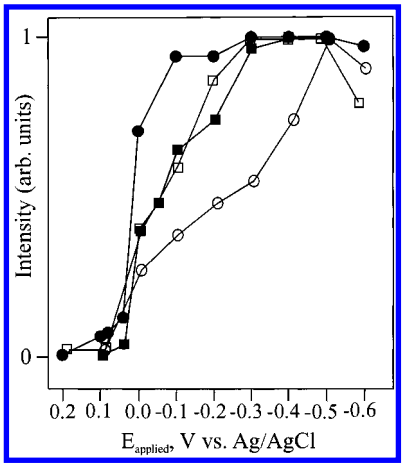

Figure 10. SERRS-detected steady state voltammetry for electrostatically and covalently bound AgFON/6-MHA/Fe^{2+}Cc and AgFON/11-MUA/1-O*T*/Fe^{2+}Cc surfaces as monitored by the intensity of the1225 cm^{-1} mode. (●) Electrostatic binding, 6-MHA; (■) covalent binding, 6-MHA; (□) covalent binding, 11-MUA/1-OT; and (○) electrostatic binding, 11-MUA/1-OT. Experimental conditions: 8 mW at $\lambda_{ex} = 514.5$ nm, 1×10^{-6} M Fe^{2+}Cc in 4.4 mM KPi, pH 7.0, -0.60 V $\leq E_{applied}$ vs Ag/AgCl $\leq +0.20$ V.

$Cc]_{surf} < 0.001$. Similarly, when $E_{applied} \leq +0.10$ V versus Ag/AgCl the electrostatically bound Cc is completely oxidized and the ratio of the surface concentrations of oxidized to reduced Cc is $[Fe^{3+}Cc]_{surf}/[Fe^{2+}Cc]_{surf} > 1000$. Since SERR intensities are approximately proportional to surface concentration, the ratio $[Fe^{3+}Cc]_{surf}/[Fe^{2+}Cc]_{surf}$ that corresponds to each value of $E_{applied}$ can be calculated from

$$\frac{[Fe^{3+}Cc]_{surf}}{[Fe^{2+}Cc]_{surf}} = \frac{(1 - I^{norm}_{1225cm^{-1}})}{(I^{norm}_{1225cm^{-1}})} \qquad (2)$$

where $I^{norm}_{1225cm^{-1}}$ is the SERR intensity of the 1225 cm^{-1} mode of Fe^{2+}Cc normalized to 1 at $E_{applied} = -0.4$ V versus Ag/AgCl. The slope of the SERRS-detected Nernst plot in Figure 9 is 61 mV per decade change of the ratio of the surface concentrations. This compares favorably to the 59 mV value expected for a reversible one electron-transfer reaction. This is a significant result because reversible electrochemistry indicates that the bound molecule has retained its biological function and is not denatured at the electrode surface.

The surface formal potential $E^{0'}$ for the electrostatically adsorbed Cc redox couple determined from Figure 9 was $E^{0'} = -0.014$ V vs Ag/AgCl or, using the conversion factor $E_{Ag/AgCl} = +0.197$ V vs normal hydrogen electrode (NHE), $E^{0'} = +0.183$ V vs NHE. The SERRS-detected surface formal potential can be compared with that determined by electrochemical studies of Cc on carboxylic acid terminated SAM modified Au electrodes.[21,22] Our value of $E^{0'} = +0.183$ V vs NHE is remarkably comparable to the value of 190 mV obtained by Collinson et al.[22] on a similar surface. For comparison, the solution value is $E^{0'} = +0.260$ V vs NHE.[94] These results are also consistent with the conclusion that biological function is retained in Cc electrostatically bound to the AgFON/6-MHA surface.

Distance and Orientation Dependence of Heterogeneous ET between Fe^{2+}Cc and AgFON/SAM Surfaces. We now return to the SERRS-detected steady-state voltammetry for the oxidation and rereduction of Fe^{2+}Cc electrostatically bound to the 11-MUA/AgFON electrode surface. Initially, SERRS could not be observed for 11-MUA/AgFON surfaces; however, by forming a mixed monolayer with a shorter methyl-terminated alkanethiol, 1-OT, high signal-to-noise ratio SERR spectra of electrostatically bound Fe^{2+}Cc were obtained. It is likely that the 1-OT chains promote ionization of the carboxylic acid groups of 11-MUA/AgFON by (1) disrupting the hydrogen bonding between neighboring COOH groups and (2) reducing the electrostatic repulsion between neighboring COO^- groups.

Figure 10 shows the SERRS-detected steady-state voltammogram for the oxidation and rereduction of Fe^{2+}Cc electrostatically bound to the mixed monolayer AgFON/11-MUA/1-OT electrode surface (open circles) as monitored by the SERR intensity of the ν_{13} (B_{1g}) mode at 1225 cm^{-1}. The corresponding data for the AgFON/6-MHA electrode surface (filled circles) from Figure 8B has been added to Figure 10 for comparison purposes. In addition, Figure 10 shows the SERRS-detected voltammetry for Fe^{2+}Cc covalently cross-linked to both AgFON/6-MHA (filled squares) and AgFON/11-MUA/1-OT (open squares) electrode surfaces. When Fe^{2+}Cc is covalently bound to the surface, the possibility of desorption due to potential changes is eliminated. Therefore, the decrease in the SERR signal intensity as $E_{applied}$ is scanned anodically cannot be due to protein desorption. We interpret this result to indicate that SERR intensity decreases solely as a consequence of the smaller extinction coefficient for Q-band electronic absorption in Fe^{3+}-Cc as compared to Fe^{2+}Cc at $\lambda_{ex} = 514.5$ nm. These results convincingly demonstrate that Fe^{2+}Cc electrostatically bound to the $x = 5$ AgFON/$S(CH_2)_xCOOH$ surface exhibits reversible oxidation to Fe^{3+}Cc, whereas Fe^{2+}Cc electrostatically bound to the $x = 10$ surface exhibits irreversible oxidation. Fe^{2+}Cc covalently cross-linked to the $x = 5$ and $x = 10$ surfaces both exhibit surface electrochemistry with a similar but intermediate degree of reversibility. The result that surface electrochemistry is most reversible for the electrostatically bound AgFON/6-MHA/Fe^{2+}Cc system is extremely important because it demonstrates the important interplay between the distance dependence and the rotational orientation dependence of electron transfer to biomolecules. Our results are consistent with the distance dependence studies of ET kinetics on ferrocene and ferrocenylcarboxy terminated SAMs which found that ET rate constants exponentially decrease as $\exp(-kx)$ where the constant $k \sim 1.1$.[95,96]

Another consequence of the work reported here is that these results imply the existence of at least two design criteria for fabricating surfaces that exploit the electron-transfer interface between biology and electronics. The redox center of the surface-bound biomolecule must have both (1) a short separation

distance from the electrode surface and (2) the proper orientation to provide for efficient electron transfer.

Conclusions

The SERRS, SERRS-detected binding titrations, and SERRS-detected steady-state voltammetry results presented here demonstrate that the reversibility of the heterogeneous electron-transfer reaction between Fe^{2+}Cc and AgFON/S$(CH_2)_x$COOH surfaces depends on both the distance between the redox center and the electrode surface and their relative orientations. We presented and discussed four new features concerning the interfacial structure and electrochemical function of Fe^{2+}Cc electrostatically bound to AgFON/S$(CH_2)_x$COOH ($x = 5$, 10): (1) the heme is highly oriented with its edge directed toward the electrode surface; (2) the electrostatic association binding constants were $K = 5.0 \times 10^6\ M^{-1}$ ($x = 5$) and $1.1 \times 10^6\ M^{-1}$ ($x = 10$); (3) fully reversible oxidation to ferricytochrome *c* (Fe^{3+}Cc) was found for the $x = 5$ system, whereas it was irreversible for $x = 10$; and (4) the Nernst slope and surface formal potential for the AgFON/S$(CH_2)_x$COOH/Fe^{3+}Cc ($x = 5$) + $1e^- \rightleftarrows$ AgFON/S$(CH_2)_x$COOH/Fe^{2+}Cc ($x = 5$) reaction were 61 mV and $E^{0'} = +0.183$ V vs NHE, respectively. From these results, we are drawn to the conclusion that AgFON/S$(CH_2)_x$COOH surfaces are biocompatible with electrostatically bound Fe^{2+}Cc in that its native structure and biological function are preserved. Furthermore, we conclude that AgFON/S$(CH_2)_x$COOH surfaces are biomimetic to the extent that the association binding constants are of comparable magnitude to that of the prototypical interprotein electron-transfer complex Cc−CcP.

Similar SERRS spectroelectrochemistry experiments were carried out to probe the interfacial structure and electrochemical function of the corresponding AgFON/S$(CH_2)_x$COOH surfaces to which Fe^{2+}Cc was covalently cross-linked by amide bond formation. These results established that (1) the heme is randomly oriented with no preferred direction between the heme edge and the electrode surface and (2) the oxidation to Fe^{3+}Cc exhibited the same degree of reversibility for $x = 5$ and $x = 10$; but was intermediate between the $x = 5$ and $x = 10$ electrostatically bound cases. Covalent cross-linking between Fe^{2+}Cc and AgFON/S$(CH_2)_x$COOH surfaces does not result in a fully biomimetic system.

Finally, we point out an important practical significance of these SERRS spectroelectrochemistry experiments that extends beyond the specifics of the AgFON/S$(CH_2)_x$COOH/Fe^{2+}Cc system. We demonstrated here, for the first time, that AgFON/S$(CH_2)_x$COOH surfaces have SERRS enhancement factors that are stable to a wide range of ionic strength, pH, electrolyte, and redox potential variations. This stability enables SERRS studies of adsorbed biomolecules as a function of these important biophysical variables which have not been accessible, heretofore, with either colloid or AgORC surfaces. The biomimetic/biocompatible character of these AgFON/S$(CH_2)_x$COOH surfaces coupled with their unusual stability and large surface enhancement factors greatly extends the usefulness of SERRS in the study of surface-confined biomolecules.

Acknowledgment. We gratefully acknowledge NSF (Grant CHE-940078) for financial support. For supplying purified cytochrome *c*, we thank Michael DeVan and Eric Stemp. We also thank the Hoffman synthetic subgroup at Northwestern University for their assistance in the synthesis and characterization of mercaptocarboxylic acids.

References and Notes

(1) Cotton, T. M.; Kim, J.-H.; Chumanov, G. D. *J. Raman Spectrosc.* **1991**, *22*, 729−742.
(2) Fabian, H.; Anzenbacher, P. *Vib. Spectrosc,* **1993**, *4*, 125−148.
(3) Nabiev, I.; Chourpa, I.; Manfait, M. *J. Raman Spectros.* **1994**, *25*, 13−23.
(4) Cotton, T. M.; Schultz, S. G.; Van Duyne, R. P. *J. Am. Chem. Soc.* **1980**, *102*, 7960−7962.
(5) Smulevich, G.; Spiro, T. G. *J. Phys. Chem.* **1985**, *89*, 5168−5173.
(6) Copeland, R. A.; Fodor, S. P. A.; Spiro, T. G. *J. Am. Chem. Soc.* **1984**, *106*, 3872−3874.
(7) Broderick, J. B.; Natan, M. J.; O'Halloran, T. V.; Van Duyne, R. P. *Biochemistry* **1993**, *32*, 13771−13776.
(8) de Groot, J.; Hester, R. E. *J. Phys. Chem.* **1988**, *92*, 2044−2048.
(9) Verma, A. L.; Kimura, K.; Yagi, T.; Nakamura, A.; Inokuchi, H.; Kitagawa, T. *Chem. Phys. Lett.* **1989**, *159*, 189−192.
(10) Keating, C. D.; Kovaleski, K. M.; Natan, M. J. *J. Phys. Chem. B* **1998**, *102*, 9404−9413.
(11) Keating, C. D.; Kovaleski, K. K.; Natan, M. J. *J. Phys. Chem. B* **1998**, *102*, 9414−9425.
(12) Pachence, J. M.; Blasie, J. K. *Biophys. J.* **1987**, *52*, 735−747.
(13) Amador, S. M.; Pachence, J. M.; Fischetti, R.; McCauley, J. P. J.; Smith, A. B., III.; Blasie, J. K. *Langmuir* **1993**, *9*, 812−817.
(14) Sagara, T.; Niwa, K.; Sone, A.; Hinnen, C.; Niki, K. *Langmuir* **1990**, *6*, 254−262.
(15) Feng, Z. Q.; Imabayashi, S.; Kakiuchi, T.; Niki, K. *J. Electroanal. Chem.* **1995**, *394*, 149−154.
(16) Bustamante, C.; Vesenka, J.; Tang, C. L.; Rees, W.; Guthold, M.; Keller, R. *Biochemistry* **1992**, *31*, 22−26.
(17) Bottomley, L. A.; Haseltine, J. N.; Allison, D. P.; Warmack, R. J.; Thundat, T.; Sachleben, R. A.; Brown, G. M.; Woychik, R. P.; Jacobson, K. B.; Ferrell, T. L. *J. Vac. Sci. Technol. A* **1992**, *10*, 591−595.
(18) Prime, K. L.; Whitesides, G. M. *Science* **1991**, *252*, 1164−1167.
(19) Tengvall, P.; Lestelius, M.; Liedberg, B.; Lundström, I. *Langmuir* **1992**, *8*, 1236−1238.
(20) Tarlov, M. J.; Bowden, E. F. *J. Am. Chem. Soc.* **1991**, *113*, 1847−1849.
(21) Song, S.; Clark, R. A.; Bowden, E. F.; Tarlov, M. J. *J. Phys. Chem.* **1993**, *97*, 6564−6572.
(22) Collinson, M.; Bowden, E. F.; Tarlov, M. J. *Langmuir* **1992**, *8*, 1247−1250.
(23) Rivera, M.; Wells, M. A.; Walker, F. A. *Biochemistry* **1994**, *33*, 2161−2173.
(24) Nahir, T. M.; Bowden, E. F. *J. Electroanal. Chem.* **1996**, *410*, 9−13.
(25) Cheng, J.; Terrettaz, S.; Blankman, J. I.; Miller, C. J.; Dangi, B.; Guiles, R. D. *Isr. J. Chem.* **1997**, *37*, 259−266.
(26) Clark, R. A.; Bowden, E. F. *Langmuir* **1997**, *13*, 559−565.
(27) Kasmi, A. E.; Wallace, J. M.; Bowden, E. F.; Binet, S. M.; Linderman, R. J. *J. Am. Chem. Soc.* **1998**, *120*, 225−226.
(28) Avila, A.; Gregory, B. W.; Niki, K.; Cotton, T. M. *J. Phys. Chem. B* **2000**, *104*, 2759−2766.
(29) Fragneto, G.; Thomas, R. K.; Rennie, A. R.; Penfold, J. *Science* **1995**, *267*, 657−660.
(30) Wang, J.; Wallace, C. J. A.; Clark-Lewis, I.; Caffrey, M. *J. Mol. Biol.* **1994**, *237*, 1−4.
(31) Wang, J.; Caffrey, M. *J. Am. Chem. Soc.* **1995**, *117*, 3304−3305.
(32) Willner, I.; Katz, E.; Riklin, A.; Kasher, R. *J. Am. Chem. Soc.* **1992**, *114*, 10965−10966.
(33) Kinnear, K. T.; Monbouquette, H. G. *Langmuir* **1993**, *9*, 2255−2257.
(34) Plant, A. L. *Langmuir* **1999**, *15*, 5128−5135.
(35) Hong, H.-G.; Jiang, M.; Sligar, S. G.; Bohn, P. W. *Langmuir* **1994**, *10*, 153−158.
(36) Herr, B. R.; Mirkin, C. A. *J. Am. Chem. Soc.* **1994**, *116*, 1157−1158.
(37) Stranick, S. J.; Parikh, A. N.; Tao, Y.-T.; Allara, D. L.; Weiss, P. S. *J. Phys. Chem.* **1994**, *98*, 7636−7646.
(38) Bryant, M. A.; Pemberton, J. E. *J. Am. Chem. Soc.* **1991**, *113*, 3629−3637.
(39) Troughton, E. B.; Bain, C. D.; Whitesides, G. M.; Nuzzo, R. G.; Allara, D. L.; Porter, M. D. *Langmuir* **1988**, *4*, 365−385.
(40) Smith, E. L.; Porter, M. D. *J. Phys. Chem.* **1993**, *97*, 8032−8038.
(41) Laibinis, P. E.; Whitesides, G. M.; Allara, D. L.; Tao, Y.-T.; Parikh, A. N.; Nuzzo, R. G. *J. Am. Chem. Soc.* **1991**, *113*, 7152−7167.
(42) Van Duyne, R. P.; Hulteen, J. C.; Treichel, D. A. *J. Chem. Phys.* **1993**, *99*, 2101−2115.
(43) Dick, L. A.; Van Duyne, R. P. *Anal. Chem.* **2000**. In preparation.
(44) Lecomte, S.; Hildebrandt, P.; Soulimane, T. *J. Phys. Chem. B* **1999**, *103*, 10053−10064.
(45) Wackerbarth, H.; Klar, U.; Gunther, W.; Hildebrandt, P. *Appl. Spectrosc.* **1999**, *53*, 283−291.
(46) Lecomte, S.; Wackerbarth, H.; Soulimane, T.; Buse, G.; Hildebrandt, P. *J. Am. Chem. Soc.* **1998**, *120*, 7381−7382.
(47) Terrettaz, S.; Cheng, J.; Miller, C. J.; Guiles, R. D. *J. Am. Chem. Soc.* **1996**, *118*, 7857−7858.

(48) Hu, S.; Morris, I. K.; Singh, J. P.; Smith, K. M.; Spiro, T. G. *J. Am. Chem. Soc.* **1993**, *115*, 12446−12458.
(49) Li, X.-Y.; Czernuszewicz, R. S.; Kincaid, J. R.; Stein, P.; Spiro, T. G. *J. Phys. Chem.* **1990**, *94*, 47−61.
(50) Koppenol, W. H.; Margoliash, E. *J. Biol. Chem.* **1982**, *257*, 4426−4437.
(51) Bushnell, G. W.; Louie, G. V.; Brayer, G. D. *J. Mol. Biol.* **1990**, *214*, 585−595.
(52) Wirth, M. J.; Fairbank, R. W. P.; Fatunmbi, H. O. *Science* **1997**, *275*, 44−47.
(53) Keller, S. W.; Kim, H.-N.; Mallouk, T. E. *J. Am. Chem. Soc.* **1994**, *116*, 8817−8818.
(54) Willit, J. L.; Bowden, E. F. *J. Phys. Chem.* **1990**, *94*, 8241−8246.
(55) Niaura, G.; Gaigalas, A. K.; Vilker, V. L. *J. Electroanal. Chem.* **1996**, *416*, 167−178.
(56) Quaroni, L.; Reglinski, J.; Wolf, R.; Smith, W. E. *Biochim. Biophys. Acta* **1996**, *1296*, 5−8.
(57) Macdonald, I. D. G.; Smith, W. E. *Langmuir* **1996**, *12*, 706−713.
(58) Eng, L. H.; Schlegel, V.; Wang, D.; Neujahr, H. Y.; Stankovich, M. T.; Cotton, T. M. *Langmuir* **1996**, *12*, 3055−3059.
(59) Rospendowski, B. N.; Schlegel, V. L.; Holt, R. E.; Cotton, T. M. Surface Enhanced Resonance Raman Scattering from Cytochrome *c* and P-450 on Bare and Phospholipid-Coated Silver Substrates. In *Charge and Field Effects in Biosystems-2*; Allen, M. J.; Cleary, S. F.; Hawkridge, F. M., Eds.; Plenum Press: New York, 1989; pp 43−58.
(60) Virdee, H. R.; Hester, R. E. *Laser Chem.* **1988**, *9*, 401−416.
(61) Hildebrandt, P.; Pielak, G.; Williams, R. J. P. *Eur. J. Biochem.* **1991**, *30*, 211−216.
(62) Hildebrandt, P.; Heimburg, T.; Marsh, D. *Eur. Biophys. J.* **1990**, *18*, 193−201.
(63) Wolf, C. R.; Miles, J. S.; Seilman, S.; Burke, M. D.; Rospendowski, B. N.; Kelly, K.; Smith, W. E. *Biochemistry* **1988**, *27*, 1597−1603.
(64) Niki, K.; Kawasaki, Y.; Kimura, Y.; Higuchi, Y.; Yasuoka, N. *Langmuir* **1987**, *3*, 982−986.
(65) Hildebrandt, P.; Stockburger, M. *J. Phys.Chem.* **1986**, *90*, 6017−6024.
(66) Hobara, D.; Niki, K.; Cotton, T. M. *Biospectroscopy* **1998**, *4*, 161−170.
(67) Brautigan, D. L.; Ferguson-Miller, S.; Margoliash, E. *Methods Enzymol.* **1978**, *53*, 128−164.
(68) Miller, B. E. Surface Enhanced Raman Scattering On Composition Modulated Alloys and Surface and Solution Raman Scattering in the Visible and Ultraviolet. Dissertation, Northwestern University, Evanston, IL, 1989.
(69) Lakovits, J. M. Part 1: Resonance Raman Spectroelectrochemistry of the Tetracyanoquinodimethane Dianion. Part 2: Double Potential Step Chronocoulometry Studies of Adsorption on a Silver Electrode. Dissertation, Northwestern University, Evanston, IL, 1981.
(70) Fornari, B.; Mattei, G.; Pagannone, M. *J. Vac. Sci. Technol. A* **1988**, *6*, 167−168.
(71) Carron, K. T. Surface Enhanced Resonance Raman, Resonance Hyper-Raman, and Hyper-Raman Spectroscopy of Molecules Adsorbed to Thin Metal Films. Dissertation, Northwestern University, Evanston, IL **1985**.
(72) Bain, C. D.; Troughton, E. B.; Tao, Y.-T.; Evall, J.; Whitesides, G. M.; Nuzzo, R. G. *J. Am. Chem. Soc.* **1989**, *111*, 321−335.
(73) Maeda, Y.; Yamamoto, H.; Kitano, H. *J. Phys. Chem.* **1995**, *99*, 4837−4841.
(74) Spiro, T. G.; Strekas, T. C. *Proc. Natil. Acad. Sci U.S.A.* **1972**, *69*, 2622−2626.
(75) Spiro, T. G. *Biological Applications of Raman Spectroscopy*; John Wiley and Sons: New York, 1988; Vol. 1−3.
(76) Hildebrandt, P.; Stockburger, M. *Biochemistry* **1989**, *28*, 6710−6721.
(77) Hildebrandt, P.; Stockburger, M. *Biochemistry* **1989**, *28*, 6722−6728.
(78) Moskovits, M. *J. Chem. Phys.* **1982**, *77*, 4408−4416.
(79) Moskovits, M.; Suh, J. S. *J. Phys. Chem.* **1984**, *88*, 5526−5530.
(80) Creighton, J. A. The Selection Rules for Surface-Enhanced Raman Spectroscopy. In *Spectroscopy of Surfaces*; Clark, R. J. H., Hester, R. E., Eds.; John Wiley & Sons Ltd.: New York, 1988; Vol. 15, pp 37−89.
(81) Moskovits, M.; DiLella, D. P.; Maynard, K. J. *Langmuir* **1988**, *4*, 67−76.
(82) Grabhorn, H.; Otto, A. *Vacuum* **1990**, *41*, 473−475.
(83) Gao, X.; Davies, J. P.; Weaver, M. J. *J. Phys. Chem.* **1990**, *94*, 6858−6864.
(84) Roy, D.; Furtak, T. E. *Chem. Phys. Lett.* **1986**, *124*, 299−303.
(85) Jianxin, Q. Y.; Sun, L. *J. Phys. Chem. B* **1997**, *101*, 8221−8224.
(86) Kennedy, B. J.; Spaeth, S.; Dickey, M.; Carron, K. T. *J. Phys. Chem. B* **1999**, *103*, 3640−3646.
(87) Bain, C. D.; Whitesides, G. M. *Langmuir* **1989**, *5*, 1370−1378.
(88) Wang, J.; Frostman, L. M.; Ward, M. D. *J. Phys. Chem.* **1992**, *96*, 5224−5228.
(89) Maeda, Y.; Kitano, H. *J. Phys. Chem.* **1995**, *99*, 487−488.
(90) Leesch, V. W. Binding and Electron Transfer between Cytochrome *c* and Cytochrome *c* Peroxidase. Ph.D. Thesis, Northwestern University, 2000.
(91) Leesch, V. W.; Bujons, J.; Mauk, A. G.; Hoffman, B. M. *Biochemistry* **2000**, *39*. In press.
(92) Dick, L. A.; Haes, A. J.; Van Duyne, R. P. *J. Phys. Chem. B* **2000**. Submitted for publication.
(93) Spiro, T. G.; Strekas, T. C. *J. Am. Chem. Soc.* **1974**, *96*, 338−345.
(94) Dickerson, R. E.; Timkovich, R.; Boyer, P. D. Cytochromes (c) In *The Enzymes*; Boyer, P. D., Ed.; Academic Press: New York, 1975; Vol. XI-A, pp 397−547.
(95) Smalley, J. F.; Feldberg, S. W.; Chidsey, C. E. D.; Linford, M. R.; Newton, M. D.; Liu, Y.-P. *J. Phys. Chem.* **1995**, *99*, 13141−13149.
(96) Carter, M. T.; Rowe, G. K.; Richardson, J. N.; Tender, L. M.; Terrill, R. H.; Murray, R. W. *J. Am. Chem. Soc.* **1995**, *117*, 2896−2899.